Decoupling Controller of PVC Stripping Process Based on Subspace Modeling

Hao-Ming Song, Wei-Zhong Sun*, Jie-Sheng Wang, Lei Zhang

Abstract—**Based on the basic principle of PVC stripping process, the subspace modeling method, the decoupling method of muti-variable coupling system and PID controller parameter setting method, a decoupling control method of PVC stripping process based on subspace modeling is proposed. Then the subspace modeling method was used to model top temperature-slurry flow and bottom temperature-steam flow in the PVC stripping process. The diagonal matrix decoupling and feed-forward compensation decoupling methods are used to decouple the TITO system to obtain two SISO systems, which are controlled by two PID controllers respectively. PID parameters are tuned by using four engineering tuning methods to obtain the step response curves. For different controlled objects, four PID controller parameter adjustment methods will show different effects.**

Index Terms—**PVC stripping process; Subspace modeling; Decoupling control; PID controller**

I. Introduction

PVC (Polyvinyl chloride) is a substance formed by the polymerization of Vinyl chloride monomer (called VCM) through free radicals acted by light and heat. Vinyl chloride has a wide range of uses: vinylidene chloride, acrylonitrile, acrylates, and other monomers can be copolymerized with vinyl chloride to form copolymers, and can also be used as refrigerants [1]. Polyvinyl chloride (PVC) was the first product to be put into industrial production and is the most widely used polymer. Due to its stability, non-flammability, good weather resistance and high strength, it immobilizes a quarter of the chlorine in the world, making a positive contribution to environmental optimization [2]. With the increase of chemical equipment, PVC production process control requirements are becoming more and more stringent. The production process of PVC mainly involves polymerization, stripping and rectification, and the process is complex. In different processes of production, production indicators should be strictly controlled, otherwise safety events may be triggered [3]. Among them, the conversion rate of vinyl chloride (VCM) will directly affect the quality of PVC products. Polyvinyl chloride is formed by the free radical polymerization of vinyl chloride, the main method is through suspension polymerization, the PVC produced by this method accounts for 80% of the total output. Among them, vinyl chloride monomer is mainly obtained by ethylene, petroleum and calcium carbide processes [4].

The development of computer technology and intelligent control technology provides a better solution to solve the control problems encountered in the production process of PVC, and provides a lot of technical support for the traditional modeling problems. Due to the emergence of intelligent control technology, the production efficiency has been greatly improved. After the 1990s, many experts and scholars at home and abroad have widely adopted intelligent control technology in the production process of PVC [5]. In the process of research, Marusak et al. adopted fuzzy logic in the manufacturing method of insulated wire, aiming to control the temperature of PVC material based on the principle of fuzzy logic, so as to promote the production process without manual supervision and control [6-7]. Tian et al. proposed a nonlinear hybrid modeling method, the main purpose of which was to improve model performance and robustness of new data in the optimal control of batch MMA polymerization reactors [8]. Ye et al. mainly analyzed the temperature of the aggregator, and found that it was controlled by mixing hot and cold water, and the delay characteristic was very serious. In face of these problems, based on GPC, a cascade control method for the temperature of the aggregator was developed. According to the experimental results, this method can produce good control effect [9]. Manenti et al. mainly analyzed the polymerization principle of polyethylene terephthalate and built an advanced predictive control model based on it, which not only contains algebraic equations but also consists of 1500 difference equations, greatly improving the control accuracy of polymerization [10].

Nowadays, among several technologies to remove VCM monomer residue in PVC slurry, stripping is the most widely used and most efficient process. This process not only has great coupling and nonlinear characteristics, but also has small time-varying and other related characteristics. The whole process is complicated and non-linear, so the expected effect cannot be achieved through conventional modeling [11-12]. After analyzing the stripping process, it is found that it is in essence a process with characteristics such as nonlinear, strong coupling and time-varying, and its accurate mathematical model is difficult to determine, and it is difficult to obtain good control effects by using traditional

Manuscript received November 1, 2023; revised March 10, 2024. This work was supported by the Basic Scientific Research Project of Institution of Higher Learning of Liaoning Province (Grant No. LJKZ0293), and Postgraduate Education Reform Project of Liaoning Province (Grant No. LNYJG2022137).

Hao-Ming Song is a doctoral student of School of Electronic and Information Engineering, University of Science and Technology Liaoning, Anshan, 114051, P. R. China (e-mail: 823234806@qq.com).

Wei-Zhong Sun is a lecturer of School of Computer Science and Software Engineering, University of Science and Technology Liaoning, Anshan, 114051, P. R. China (Corresponding author, phone: 86-0412-2538246; fax: 86-0412-2538244; e-mail: lnkdswz@126.com).

Jie-Sheng Wang is a professor of School of Electronic and Information Engineering, University of Science and Technology Liaoning, Anshan, 114051, P. R. China (e-mail: wang_jiesheng@126.com).

Lei Zhang is an undergraduate student of School of Electronic and Information Engineering, University of Science and Technology Liaoning, Anshan, 114051, P. R. China (e-mail: zl1764066@163.com).

control methods [13]. In this paper, according to the relationship between the stripper process and variables, the actual operation data of the process and the subspace modeling method are selected to construct the corresponding mathematical model, and a double-input and double-output system is obtained, that is, slurry flow-tower top temperature and steam flow-tower bottom temperature. The system is effectively decoupled by using diagonal array and feed-forward compensation decoupling method. Finally, PID controller is applied to the stripping process after decoupling to realize the decoupling control of the stripping process of PVC.

II. PVC STRIPPING PROCESS

Stripping refers to the direct contact between waste water and water vapor, so that toxic and harmful substances are allocated to the gas phase to a certain extent, in order to achieve the purpose of separating pollutants. PVC resin cannot be used as the final product until the residual vinyl chloride monomer is removed. The stripping stage of PVC is completed in a suspension stripping tower, after which it can be dried for packaging. In the PVC suspension to be treated, its mass fraction is usually maintained within 25%-30%, VCM is in the range of 2%-4%, the other components are water, and the distribution ratio of VCM in the three states is about 1:10000:100. It is precisely because of the uneven distribution in the three states that the slurry side has a certain diffusion concentration gradient and dissociation power. In the slurry, VCM in the solid state must be transferred from the side with higher concentration to the side with lower concentration through the gap between PVC particles, regardless of the analysis or diffusion operation, but the solubility of VCM in water often changes with the decrease and increase of temperature [14]. Under a certain temperature condition, the VCM contained in water will dissolve, and the VCM emanating from PVC to water will break the resistance, thus diffusing into the gaseous state. Heat is exchanged with the slurry to increase its temperature, so that the VCM in it can be resolved.

PVC slurry is transported to the receiving tank by the polymerization kettle to recover the vinyl chloride in it, the slurry is filtered and the slurry after stripping out of the bottom of the tower to carry out heat exchange operation, and then transferred into the top position of the stripping tower, PVC slurry will be sprayed to the stripping tray by the nozzle, and then from the bottom end along the space in the stripping tower version of the flow from top to bottom. The low-pressure steam flows from the bottom of the stripper tower along the gap on the stripper plate from bottom to bottom, and counter-current contact occurs with the PVC slurry in the descending process. At this time, heat and mass transfer reactions occur, and the residual vinyl chloride is resolved [15]. The top of the stripper will discharge steam and resolved vinyl chloride monomer, which will be transferred to the condensing tank after condensation operation. When condensate separation is started, the liquid level control operation of the tank will be opened simultaneously. The centrifugal mother liquor water recovery equipment will receive excess condensate water, and the vinyl chloride gas cabinet will store vinyl chloride monomer. The stripping process of PVC is shown in Fig. 1.

The reasons that affect the stable operation of the PVC stripper usually involve the temperature, steam and slurry flow, pressure, liquid level difference and so on. Table I shows the control parameter values used during striping of a certain specification resin. The analysis shows that the stripping process of PVC has strong nonlinear and the coupling relationship between multiple variables is quite serious. The top and bottom temperatures usually have a great impact on the stripping process, and the steam and slurry flow rate are the two most important control variables among many variables that directly affect the stripping column. Although the number of control variables is not large, there is no more effective mathematical model, it is difficult to establish the strong coupling relationship between different variables, so it is difficult to create a better performance of the control model. In this paper, subspace modeling and PID control strategy after decoupling are proposed for the stripping process of PVC.

III. PVC STRIPPING PROCESS SUBSPACE MODELING

A. Subspace Modeling

At present, the application of subspace identification method to modeling of complex industrial processes, which is difficult to establish mechanism and empirical model, has been widely concerned. Subspace identification technology does not need the prior knowledge of the system, and can directly use the input and output data to obtain the dynamic model of the system through the ideas of statistics, optimization and linear algebra. It can effectively avoid the shortcomings of the traditional modeling process, which is expensive, complex calculation and narrow application range, so it has universal applicability and application value.

TABLE I. CONTROL VALUES TO STRING TOWER PARAMETERS

Control point name	Radius	Alarm range		Range of normal values	Actual value
Tower top temperature	0-150℃	Upper limit：110℃	Lower limit：70℃	80-105℃	85℃
Tower bottom temperature	0-150℃	Upper limit：130℃	Lower limit：100℃	105-113℃	107℃
Overhead pressure	0-0.1 MPa	Upper limit：0.08 MPa	Lower limit：0.02 MPa	0.03-0.06 MPa	0.03 MPa
Column pressure differential	0-60 MPa	Upper limit：30 MPa	Lower limit：5 MPa	10-25 MPa	15 MPa
Steam flow	0-4000 kg/h	Upper limit：3500kg/h	Lower limit：1000kg/h	1500-3000kg/h	2200 kg/h
Slurry flow	0-80 m^3/h	Upper limit：70 m^3/h	Lower limit：15m^3/h	35-50 m^3/h	40-45m^3/h
Column steam pressure	0-0.6 MPa	Upper limit：0.5 MPa	Lower limit：0.15 MPa	0.35-0.4 MPa	0.38 MPa

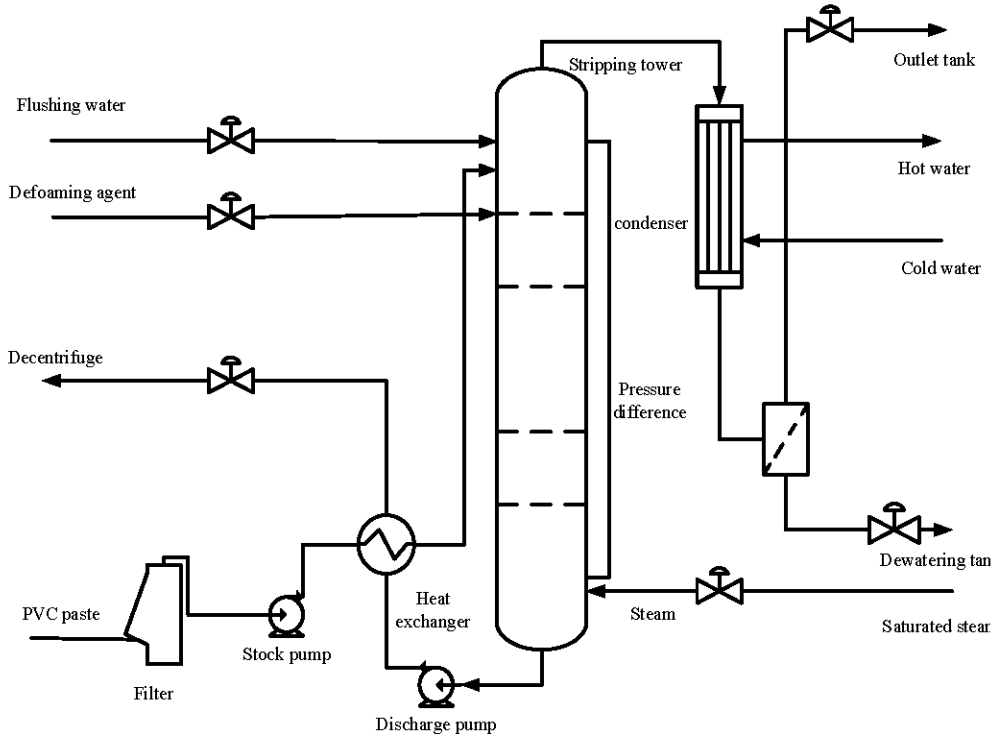

Fig. 1 Flowchart of PVC stripping process.

N4SID algorithm based on mathematical model is accurate and simple for the identification of MIMO system. The model constructed by N4SID subspace identification method has stronger anti-interference ability and good fast performance [16]. In the design and operation of model-based control systems, the quality of the model is particularly important. First, with the rapid development of the process industry, the accuracy standards set on the relevant process models are increasing year by year, and it is becoming more and more difficult to construct complex process models using mechanism methods. Second, due to simple changes in operating conditions and sensitivity to changes in the actual production process, the parameters of the real model will change over time, and the mismatch of the model will appear, and the model is inaccurate. The subspace recognition method can directly establish the equation of state of the system space with multiple entrances, so it has attracted wide attention of researchers. In this chapter, N4SID algorithm combined with field data is used to model the stripping process of PVC, which has practical significance to improve the accuracy and efficiency of the process model. Consider the linear time-invariant state space model as follows:

$$\begin{aligned} x_{k+1} &= Ax_k + Bu_k \\ y_k &= Cx_k + Du_k \end{aligned} \tag{1}$$

where, $x_k \in \mathrm{R}^n, u_k \in \mathrm{R}^m$ and $y_k \in R^l$ in turn represents the state vector, input observation vector and output observation vector of the process at time k. The defining symbol of Eq. (1) is set as past input/output Hankle matrix.

$$U_{\mathrm{p}} = \begin{bmatrix} u(0) & u(1) & \cdots & u(N-1) \\ u(1) & u(2) & \cdots & u(N) \\ \vdots & \vdots & \ddots & \vdots \\ u(k-1) & u(k) & \cdots & u(k+N-2) \end{bmatrix} \tag{2}$$

$$Y_p = \begin{bmatrix} y(0) & y(1) & \cdots & y(N-1) \\ y(1) & y(2) & \cdots & y(N) \\ \vdots & \vdots & \ddots & \vdots \\ y(k-1) & y(k) & \cdots & y(k+N-2) \end{bmatrix} \tag{3}$$

Future input/output Hankle matrix can be expressed:

$$U_{\mathrm{f}} = \begin{bmatrix} u(k) & u(k+1) & \cdots & u(k+N-1) \\ u(k+1) & u(k+2) & \cdots & u(k+N) \\ \vdots & \vdots & \ddots & \vdots \\ u(2k-1) & u(2k) & \cdots & u(2k+N-2) \end{bmatrix} \tag{4}$$

$$Y_{\mathrm{f}} = \begin{bmatrix} y(k) & y(k+1) & \cdots & y(k+N-1) \\ y(k+1) & y(k+2) & \cdots & y(k+N) \\ \vdots & \vdots & \ddots & \vdots \\ y(2k-1) & y(2k) & \cdots & y(2k+N-2) \end{bmatrix} \tag{5}$$

Toeplitz Matrix can be represented as:

$$\Psi_k = \begin{bmatrix} D & 0 & \cdots & 0 \\ CB & D & \cdots & 0 \\ \vdots & \vdots & \ddots & \vdots \\ CA^{k-2}B & CA^{k-3}B & \cdots & D \end{bmatrix} \tag{6}$$

Then obtain the extended observability matrix:

$$\Gamma_k = \begin{bmatrix} C \\ CA \\ \vdots \\ CA^{k-1} \end{bmatrix} \tag{7}$$

Past state sequence can be expressed as:

$$X_{\mathrm{p}} = \begin{bmatrix} x(0) & x(1) & \cdots & x(N-1) \end{bmatrix} \tag{8}$$

So obtain the future state sequence:

$$X_{\mathrm{f}} = \begin{bmatrix} x(k) & x(k+1) & \cdots & x(k+N-1) \end{bmatrix} \tag{9}$$

According to Eq. (1)-(9), get:

$$Y_{\mathrm{p}} = \Gamma_k X_{\mathrm{p}} + \psi_k U_{\mathrm{p}} \tag{10}$$

$$Y_{\mathrm{f}} = \Gamma_k X_{\mathrm{f}} + \psi_k U_{\mathrm{f}} \tag{11}$$

Define:

$$w_p = \begin{bmatrix} U_p \\ Y_p \end{bmatrix} \tag{12}$$

Consider the following lower triangular orthogonal LQ decomposition:

$$\begin{bmatrix} U_{\mathrm{f}} \\ W_{\mathrm{p}} \\ Y_{\mathrm{f}} \end{bmatrix} = \begin{bmatrix} R_{11} & 0 & 0 \\ R_{21} & R_{22} & 0 \\ R_{31} & R_{32} & R_{33} \end{bmatrix} \begin{bmatrix} Q_1^T \\ Q_2^T \\ Q_3^T \end{bmatrix} \tag{13}$$

where, R_1 and R_2 are the lower triangular matrix, $R_{33} = 0$, and Q_1 and Q_2 are orthogonal. From Eq. (13), obtain:

$$R_{22} Q_2^{\mathrm{T}} = W_{\mathrm{p}} - R_{21} Q_1^{\mathrm{T}} \tag{14}$$

$$Q_2^{\mathrm{T}} = R_{22}^{-1} \left(W_{\mathrm{p}} - R_{21} Q_1^{\mathrm{T}} \right) \tag{15}$$

It can be seen from the LQ decomposition that $Y_{\mathrm{f}} = R_{31} Q_1^{\mathrm{T}} + R_{32} Q_2^{\mathrm{T}}$, according to Eq. (15) and $Q_1^{\mathrm{T}} = R_{11}^{-1} U_{\mathrm{f}}$, it can be derived:

$$Y_{\mathrm{f}} = R_{32} R_{22}^{-1} W_{\mathrm{p}} + \left(R_{31} - R_{32} R_{22}^{-1} R_{21} \right) R_{11}^{-1} U_{\mathrm{f}} \tag{16}$$

By comparing Eq. (11) and Eq. (16), obtain:

$$\xi = R_{32} R_{22}^{-1} W_{\mathrm{p}} = \Gamma_{\mathrm{k}} X_{\mathrm{f}} \tag{17}$$

Perform SVD decomposition on ξ to get:

$$\xi = \begin{bmatrix} U_1 & U_2 \end{bmatrix} \begin{bmatrix} \Sigma_1 & 0 \\ 0 & 0 \end{bmatrix} \begin{bmatrix} V_1^{\mathrm{T}} \\ V_2^{\mathrm{T}} \end{bmatrix} = U_1 \Sigma_1 V_1^{\mathrm{T}} \tag{18}$$

$$\Gamma_k = U_1 \Sigma_1^{1/2} T, \quad |T| \neq 0 \tag{19}$$

$$X_{\mathrm{f}} = T^{-1} \Sigma_1^{1/2} V_1^{\mathrm{T}} \tag{20}$$

The state sequence vector shown in Eq. (21) can be estimated according to the above formula.

$$X_k = \begin{bmatrix} x(k) & x(k+1) & \cdots & x(k+N-1) \end{bmatrix} \tag{21}$$

Define an N-1 dimensional vector:

$$\overline{X}_{k+1} = \begin{bmatrix} x(k+1) & \cdots & x(k+N-1) \end{bmatrix} \tag{22}$$

$$\overline{X}_k = \begin{bmatrix} x(k) & \cdots & x(k+N-2) \end{bmatrix} \tag{23}$$

$$\overline{U}_{k|k} = \begin{bmatrix} u(k) & \cdots & u(k+N-2) \end{bmatrix} \tag{24}$$

$$\overline{Y}_{k|k} = \begin{bmatrix} y(k) & \cdots & y(k+N-2) \end{bmatrix} \tag{25}$$

According to the above formula, obtain:

$$\begin{bmatrix} \overline{X}_{k+1} \\ \overline{Y}_{k|k} \end{bmatrix} = \begin{bmatrix} A & B \\ C & D \end{bmatrix} \begin{bmatrix} \overline{X}_k \\ \overline{U}_{k|k} \end{bmatrix} \tag{26}$$

This is a linear matrix method in the system, so the least square method can be used to estimate the matrix parameters:

$$\begin{bmatrix} \hat{A} & \hat{B} \\ \hat{C} & \hat{D} \end{bmatrix} = \left(\begin{bmatrix} \overline{X}_{k+1} \\ \overline{Y}_{k|k} \end{bmatrix} \begin{bmatrix} \overline{X}_k \\ \overline{U}_{k|k} \end{bmatrix}^{\mathrm{T}} \right) \left(\begin{bmatrix} \overline{X}_k \\ \overline{U}_{k|k} \end{bmatrix} \begin{bmatrix} \overline{X}_k \\ \overline{U}_{k|k} \end{bmatrix}^{\mathrm{T}} \right)^{-1} \tag{27}$$

B. Modeling of Stripping Process

Collected 644 sets of data in the stripping process of PVC, double input and double output data as samples, and used N4SID to identify the stripping process data. The input data were steam flow rate and slurry flow rate; The output data is the top temperature of the stripper tower and the bottom temperature of the tower. The whole input-output data set is composed of 644*4 matrix, and the temperature model of the process system is identified from the input and output values with the help of subspace identification algorithm.

The input and output of the model are set as $U = (u_1, u_2)$ and $Y = (y_1, y_2)$, where u_1 and u_2 are steam flow rate and slurry flow rate respectively; y_1 is the top temperature of stripper tower; y_2 is the bottom temperature of the tower. The input and output matrices are identified by N4SID algorithm. The subspace system identification method can effectively identify the stripping model of PVC and establish the corresponding state space model. Function *ss2tf* in MATLAB gives the transfer function described by the state-space model, the general form is $\{num, den\} = ss2tf(A, B, C, D, iu)$, where *iu* is the transfer function of the *iu*-th input to all outputs. The stripping model is obtained as followss:

$$\begin{bmatrix} G_{11}(s) & G_{12}(s) \\ G_{21}(s) & G_{22}(s) \end{bmatrix} = \begin{bmatrix} \dfrac{2.6}{8.3s+1} e^{-0.2s} & \dfrac{-0.9}{10.4s+1} e^{-0.5s} \\ \dfrac{-1.2}{7.8s+1} e^{-0.5s} & \dfrac{1.9}{9.1s+1} e^{-0.2s} \end{bmatrix} \tag{28}$$

IV. Decoupling Control of Multi-variable Coupling System

The temperature control system belongs to a complex system which is widely used in this field. The core of temperature is to control parameters, and to ensure production quality, we must implement accurate control of temperature-related parameters. If decoupling measures are not implemented for such systems, the normal operation of each link of the system will be affected to a certain extent, and it is difficult to effectively control. Nowadays, PID debugging is more commonly used in univariable linear stationary system, but if it is applied to the temperature system with strong coupling, large delay and time-varying characteristics, the result is not satisfactory. In order to achieve the optimal control and stable operation of the temperature system, the implementation of temperature decoupling is the most effective way [17]. According to the characteristics of the temperature control system itself, the method of modeling analysis and simulation exploration, combined with diagonal matrix method and feed forward compensation method, can realize the advantages of

decoupling and PID control with high steady-state accuracy. According to the characteristics of the temperature control system, the method of modeling analysis and simulation exploration can realize the advantages of decoupling and PID control with high continuous accuracy. The decoupling control method is used to optimize and improve the control performance of the PVC stripping process control system [18]. Through decoupling, PID is used to independently control the two systems of slurry flow-stripping tower top temperature and steam flow-stripping tower bottom temperature. MATLAB simulation results show that this method can effectively overcome the coupling of temperature control system and the optimal control and stable operation of temperature system.

(1) Using the debugging operation of the relevant parameters of the controller, the accuracy characteristics of the two links can be located in different working Spaces to ensure that the coupling of the two sides is reduced. Generally speaking, the choice of this decoupling method will lead to a control loop is difficult to get good control, or even weaken its control effect.

(2) Using a decoupling control device added between the coupled output and input, it can be connected with the controlled target. In this way, the relative gain matrix of the controlled target in a broad sense can be transformed into a diagonal matrix, and then the coupling effect on different links can be cleared, that is to say, all loops are transformed into SISO control loops, and there is no coupling connection.

A. Decoupling of Diagonal Matrix

The dataset for strip surface defects is sourced from the UCI database. This dataset comprises 1941 samples, and each sample contains 27 eigenvalues. Furthermore, the dataset includes seven distinct categories of steel plate defects, namely Pastry, Z_Scratch, K_Scratch, Stains, Dirtiness, Bumps, and Other_Faults. Table I offers representative examples of data from the strip surface subsidence dataset.

As a more common decoupling method, diagonal matrix decoupling method is widely used. As far as the diagonal matrix method is concerned, it usually applies a special decoupling matrix to the channel loop, converts the parameter matrix coupled with each other, and changes it into a diagonal matrix, so as to achieve the goal of decoupling. Its standard is that the property matrix of the controlled target is multiplied by the decoupling matrix, and the diagonal matrix is obtained [19]. Fig. 2 shows the architecture diagram of polyvinyl chloride double-access double-output system using diagonal matrix method to overcome coupling between different variables. According to the design standard of diagonal matrix decoupling, we can know:

$$\begin{bmatrix} G_{11}(s) & G_{12}(s) \\ G_{21}(s) & G_{22}(s) \end{bmatrix}\begin{bmatrix} D_{11}(s) & D_{12}(s) \\ D_{21}(s) & D_{22}(s) \end{bmatrix}=\begin{bmatrix} G_{11}(s) & 0 \\ 0 & G_{22}(s) \end{bmatrix} \quad (29)$$

The output and input variables of the controlled object agree with the following matrix equation:

$$\begin{bmatrix} Y_1(s) \\ Y_2(s) \end{bmatrix}\begin{bmatrix} G_{11}(s) & 0 \\ 0 & G_{22}(s) \end{bmatrix}=\begin{bmatrix} U_{c1}(s) \\ U_{c2}(s) \end{bmatrix} \quad (30)$$

The obtained decoupling mathematical model is shown as follows:

$$\begin{bmatrix} D_{11}(s) & D_{12}(s) \\ D_{21}(s) & D_{22}(s) \end{bmatrix}=\begin{bmatrix} \frac{G_{11}(s)G_{22}(s)}{G_{11}(s)G_{22}(s)-G_{12}(s)G_{21}(s)} & \frac{-G_{22}(s)G_{12}(s)}{G_{11}(s)G_{22}(s)-G_{12}(s)G_{21}(s)} \\ \frac{-G_{11}(s)G_{21}(s)}{G_{11}(s)G_{22}(s)-G_{12}(s)G_{21}(s)} & \frac{G_{11}(s)G_{22}(s)}{G_{11}(s)G_{22}(s)-G_{12}(s)G_{21}(s)} \end{bmatrix} \quad (31)$$

By substituting the relevant data into the formula, the decoupling model can be obtained as:

$$\begin{bmatrix} D_{11}(s) & D_{12}(s) \\ D_{21}(s) & D_{22}(s) \end{bmatrix}=\begin{bmatrix} \frac{108.9s^2+46.2s+3.3}{161.4s^2+64.2s+4.8} & \frac{495s^2+264s+33}{161.4s^2+64.2s+4.8} \\ \frac{-11.55s^2-2.7s-0.15}{161.4s^2+64.2s+4.8} & \frac{108.9+46.2+3.3}{161.4s^2+64.2s+4.8} \end{bmatrix} \quad (32)$$

It can be seen from the above formula that the PVC stripping system is decomposed into two single closed-loop temperature control loops by diagonal matrix method, and individual loop control measures are implemented in turn. This method is more suitable for the temperature and humidity system where the number of variables is relatively small, while in the *N*-dimensional coupling control system, the calculation amount required by the decoupling algorithm is relatively large, and it is difficult to be effectively used in time.

B. Feed Forward Compensation Decoupling

Feed forward compensation decoupling is one of the earliest decoupling methods used to control multivariate decoupling. The feed forward compensation method is a method based on the invariant principle of automatic control, in which the input is transmitted forward and superimposed with the output of the master controller to overcome interference. The method is easy to couple, easy to implement and has remarkable effects, so it is widely used. In the single loop 1 of the coupling system, based on the function of PID controller, the input signal X_1 realizes the goal of data transfer to the output variable Y_1. It is precisely because U_1 has a coupling effect on U_2, and further decoupling U_2 feed forward compensation is carried out on U_{C2} in loop 2 [20]. The same principle is used to decouple U_{C2} feed forward compensation for U_1. If the dual-input dual-output system with temperature as a variable is analyzed, Fig. 3 shows the method of decoupling the coupling between the systems by using the feed forward compensator. The decoupling of the system can be achieved according to the principle of feed forward compensation:

$$\begin{aligned} U_{c1}G_{21}(s)+U_{c1}D_{21}(s)G_{22}=0 \\ U_{c2}G_{12}(s)+U_{c2}D_{12}(s)G_{11}=0 \end{aligned} \quad (33)$$

Therefore, the transfer function of the feed forward compensation decoupling schematic can be expressed:

$$\begin{aligned} D_{21}(s)=-G_{21}(s)-G_{22}(s) \\ D_{12}(s)=-G_{12}(s)-G_{11}(s) \end{aligned} \quad (34)$$

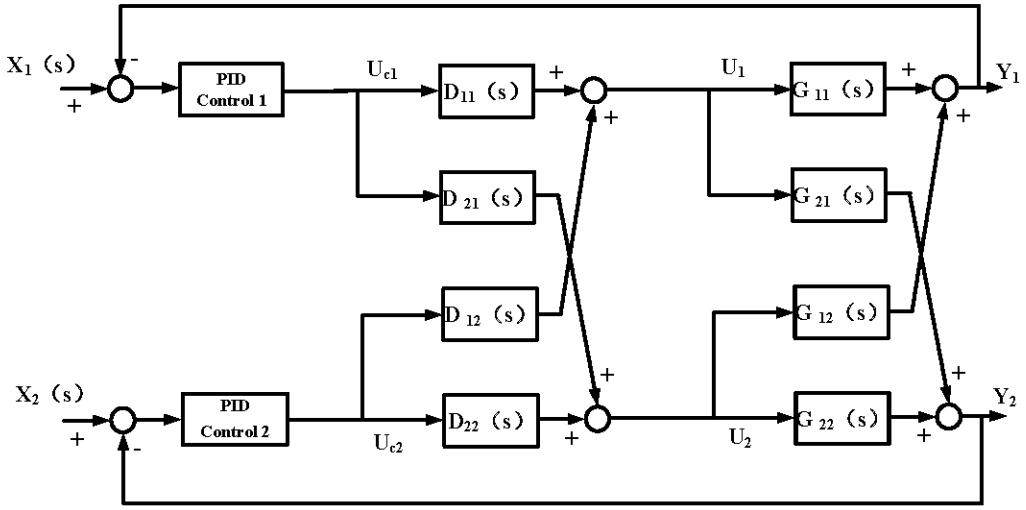

Fig. 2 Diagonal array decoupling schematic.

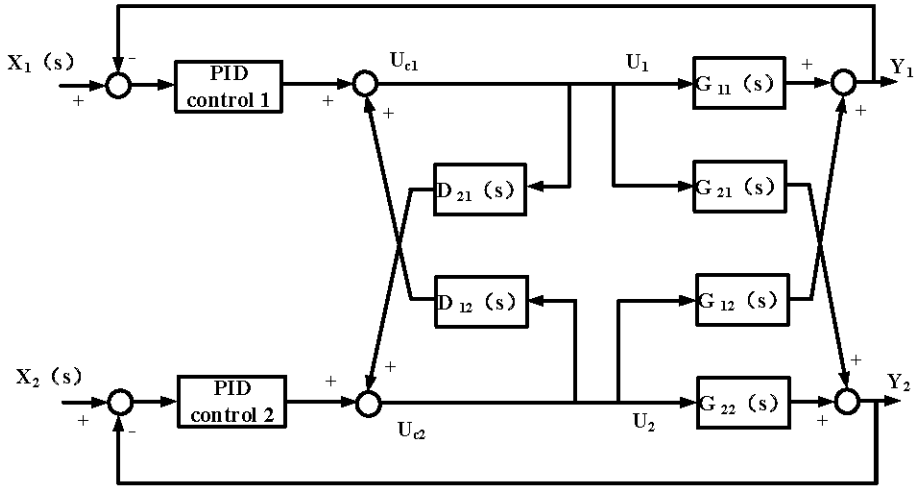

Fig. 3 Feed-forward compensation decoupling schematic.

Plug in the data and get the decoupling model:

$$\begin{aligned} D_{21}(s) &= 10.92\text{s}+1.2/14.82s+1.9 \\ D_{12}(s) &= 7.47s+0.9/27.04s+2.6 \end{aligned} \tag{35}$$

Using the feed forward compensator designed above, the two inputs can be controlled separately, thus realizing the decoupling goal of the PVC stripping process.

V. PID CONTROLLER DESIGN

A. PID Control Policy

The PID controller is based on the evaluation of "past, present and future" deviation data to further achieve efficient control algorithms. Compared with other algorithms, it simplifies the relevant process. PID controller and controlled object together constitute PID control system, system structure diagram is shown in Fig. 4. The PID controller is actually a linear controller, which constitutes a control deviation through the fixed value and the actual output value, namely:

$$e(\text{t}) = \text{r}(\text{t}) - \text{y}(\text{t}) \tag{36}$$

Then the deviation is proportional, integral and differential through the linear combination to form the control quantity, the controlled object is controlled, the ideal algorithm of PID controller is:

$$u(t) = K_p\left[e(t)+\frac{1}{T_i}\int_0^t e(t)\,\text{d}t+\frac{T_d\text{d}e(t)}{\text{d}t}\right] \tag{37}$$

where, $K_i = K_P/T_i$, $K_d = K_pT_d$, e(t) is the feedback bias. If the transfer function is used, it can be expressed as:

$$G(s) = \frac{U(s)}{E(s)} = K_p\left(1+\frac{1}{T_iS}+T_dS\right) \tag{38}$$

The value of PID controller parameters proportional gain K_p , integral time constant T_i and differential time constant T_d will affect the control effect of PID control system. Proportional gain, differential time constant and integral time constant are three important parameters of PID controller, and their values will affect the control effect of PID control system [21].

B. PID Controller Parameter Tuning Method

1) Z-N frequency response method

The critical proportionality method was developed by Ziegler J. G. and Nichols N. B. It is an engineering adjustment method that, unlike other methods, does not rely on the mathematical model of the object. The Z-N frequency response depends on the critical point above the Nye's curve of the transfer function, which is at the intersection of the Nye's curve and the negative real axis. By determining the

critical gain K_u and the critical oscillation period T_u of the controlled object, the tuning method of the Z-N critical proportionality parameters of PID is determined according to Table Ⅱ. Generally, the proportional controller is used to control the system, so that it is in a stable state and further obtain the critical point. The damping oscillation method is that the controlled system can be oscillated according to the attenuation of 4:1.

2) Cohen-Coon method

Cohen-Coon method is the model of first order inertia plus pure hysteresis. In this method, the dominant poles can be configured through related methods, so that the attenuation ratio of the system can reach 25%. For each controller has a different configuration goal, for example, when the object is a P or PD controller, the configuration goal is to increase the system's revenue and reduce the attenuation rate, and minimize the static error; When the object is a PI or PID controller, the configuration goal is to increase the integral gain value and minimize the integral error. The tuning of PID controller parameters based on Cohen-Coon method is shown in 3,where： $a=(K_pL)/T$ ， $\tau=L/(L+T)$.

3) Astrom and Hagglund method

Astrom and Hagglund is based on the relay feedback theory and forms a new PID parameter setting method, as shown in Fig. 5. In order to determine the position of the critical point, the method uses a feedback loop and adds relays to control the amplitude and frequency of the oscillation through this force, which further affects the critical gain and oscillation period. Using the above method, the stable response of the closed-loop oscillation during the control process can be determined to a large extent.

The controlled object has at least - π phase at high frequency and constant amplitude oscillation with period T, so that the controlled object's frequency phase lags behind - π , and the intersection of this frequency is the intersection of the negative real axis and the Naisley curve, then the angular frequency of the critical point here is as follows:

$$\omega_n=\frac{2\pi}{T} \tag{39}$$

μ is the amplitude of the relay characteristics, by analyzing the relay characteristics, further obtain the Fourier series expansion, the amplitude of the first item is $4\mu/\pi$, if the output of the controlled object is a , the oscillation value of y, then the amplitude of the controlled object at this point can be:

$$K_u=\frac{\pi a}{4\mu} \tag{40}$$

4) CHR tuning algorithm

After continuous development, Z-N setting method has been improved, CHR setting algorithm is one of them, in Table Ⅳ, it can be seen that the general empirical formula, including: 0% and 20% of the two overshoot, the former indicates that there can be damping, to ensure that the system in no overshoot response when the change of setting value; The latter indicates that the system can have overshoot to ensure the response to the change of the set point. Table Ⅴ gives the parameter tuning formula of PID controller with disturbance in CHR algorithm, however, 0% overshoot only acts on some control objects. Compared with Z-N tuning method, the tuning formula of CHR method does not define the critical parameter value of the system, and only uses the time constant T in the system to simplify the tuning of PID controller parameters. In Tables Ⅳ and Ⅴ, $a=\tau K/T$.

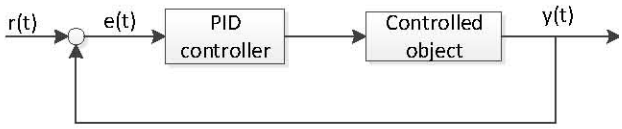

Fig. 4 PID control schematic.

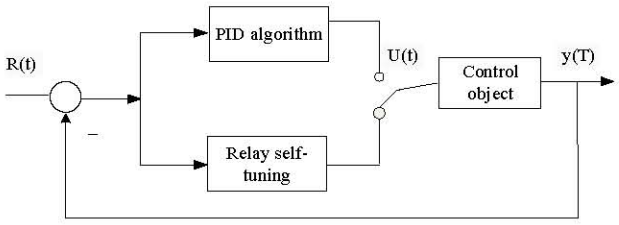

Fig. 5 Diagram of relay feedback control.

Table Ⅱ. Tuning equations of Z-N critical ratio method

PID controller parameter	K_p	T_i	T_d
P-type controller	0.5 K_u	—	—
PI type controller	0.4 K_u	0.85 T_u	—
PID type controller	0.6 K_u	0.5 T_u	0.125 T_u

Table Ⅲ. Parameter tuning formulas of Cohen-Coon method

PID Controller Parameters	K_p	T_i	T_d
P-type controller	$\frac{1}{\alpha}\left(1+\frac{0.35\tau}{1-\tau}\right)$	—	—
PI type controller	$\frac{0.9}{\alpha}\left(1+\frac{0.92\tau}{1-\tau}\right)$	$\frac{3.3-3.0\tau}{1+1.2\tau}L$	—
PID type controller	$\frac{1.35}{\alpha}\left(1+\frac{0.18\tau}{1-\tau}\right)$	$\frac{2.5-2.0\tau}{1-0.39\tau}L$	$\frac{0.37-0.37\tau}{1-0.81\tau}L$

Table Ⅳ. CHR tuning formula for set point

Type of control	There is 0% overshoot			There is 20% overshoot			Object Types
	K_p	T_i	T_d	K_p	T_i	T_d	T/R = tau
P	$0.3/\alpha$			$0.7/\alpha$			R>10
PI	$0.35/\alpha$	1.2 T		$0.6/\alpha$	T		7.5 < R < 10
PID	$0.6/\alpha$	T	0.5τ	$0.95/\alpha$	1.4 T	0.47τ	3 < R < 7.5

Table V. CHR tuning formula of perturbation point

Controller type	Has 0% overshoot			There is 20% overshoot			Object Types
	K_p	T_i	T_d	K_p	T_i	T_d	T/R = tau
P	$0.3/\alpha$			$0.7/\alpha$			R>10
PI	$0.6/\alpha$	4T		$0.7/\alpha$	2.3 T		7.5 < R < 10
PID	$0.95/\alpha$	2.4 T	0.5 τ	$1.2/\alpha$	2T	0.42 τ	3 < R < 7.5

VI. Simulation Research and Result Analysis

To validate the efficacy of the proposed methodology outlined in this research, data pertaining to the PVC stripping process is systematically gathered. The subspace modeling technique is subsequently employed to construct a comprehensive model of the PVC stripping process. Following this, two distinct decoupling methodologies are applied to achieve the intended decoupling objectives. The final phase involves the implementation of four engineering tuning methods for PID parameters to compare and regulate the decoupled system.

Within this chapter, an in-depth examination is conducted on the correlation between the temperature at the uppermost point of the stripping tower and the temperature at its base. Various decoupling techniques are systematically simulated in order to investigate their impact. Specifically, diagonal matrix decoupling results in the formulation of the following decoupling matrix:

$$\begin{bmatrix} D_{11}(s) & D_{12}(s) \\ D_{21}(s) & D_{22}(s) \end{bmatrix} = \begin{bmatrix} \dfrac{108.9s^2+46.2s+3.3}{161.4s^2+64.2s+4.8} & \dfrac{495s^2+264s+33}{161.4s^2+64.2s+4.8} \\ \dfrac{-11.55s^2-2.7s-0.15}{161.4s^2+64.2s+4.8} & \dfrac{108.9+46.2+3.3}{161.4s^2+64.2s+4.8} \end{bmatrix} \quad (41)$$

By feed forward compensation decoupling, the decoupling matrix is obtained as:

$$\begin{aligned} D_{21}(s) &= 10.92s+1.2/14.82s+1.9 \\ D_{12}(s) &= 7.47s+0.9/27.04s+2.6 \end{aligned} \quad (42)$$

Fig. 6 and Fig. 7 present simulation diagrams depicting temperature coupling at the upper and lower extremities of the tower in the absence of decoupling. Specifically, Fig. 6 illustrates the simulation diagram portraying bottom-to-top coupling, while Fig. 7 shows the simulation diagram delineating top-to-bottom coupling. Transitioning to Fig. 8 and Fig. 9, these diagrams represent the temperature coupling at the tower's extremities subsequent to the implementation of diagonal decoupling. Fig. 8 specifically encapsulates the simulation diagram depicting bottom-to-top coupling post-diagonal decoupling, while Fig. 9 corresponds to the simulation diagram illustrating top-to-bottom coupling under the same conditions. Fig. 10 and 11 delve into the realm of decoupling methodologies, each serving as a simulation diagram representing distinct approaches. Fig. 10 elucidates the simulation diagram for diagonal decoupling, while Fig. 11 offers insight into the simulation diagram for feed-forward compensation decoupling.

Seen from Fig. 12 and Fig. 13, these simulation diagrams depict the temperature coupling at the tower's upper and lower limits subsequent to decoupling with feed-forward compensation. Fig. 12 showcases the simulation diagram portraying bottom-to-top coupling, and Fig. 13 corresponds to the simulation diagram illustrating top-to-bottom coupling under the influence of feed-forward compensation decoupling.

Furthermore, Table VI comprehensively outlines the tuning parameters associated with the PID controller, while Table VII provides an exhaustive account of the performance index attributed to the PID controller. Analyzing Fig. 6-7, it is evident that in the absence of decoupling, the tower's upper section exhibits output when the temperature is set at 0,107 for both the upper and lower extremities. Conversely, when subjected to the temperature configuration (85,0) at the upper and lower extremities, output is observed at the lower portion of the tower, signifying the existence of coupling within the system.

Examining the post-diagonal decoupling results shown in Fig. 8-9, a notable shift occurs. When the temperature is set at (0,107) for the upper and lower extremities, no output is observed at the upper section, indicating the alleviation of coupling between the lower and upper portions of the tower. Similarly, when the temperature configuration (85,0) is applied, no output is discernible at the lower portion, denoting the release of coupling between the upper and lower regions of the tower.

Fig. 12-13 represent the aftermath of feed-forward compensation decoupling and further accentuate the detachment of coupling dynamics. Setting the temperature at (0,107) for the upper and lower extremities, results in Fig. 12 has no output at the upper section, denoting the liberation from bottom-to-top coupling. Similarly, applying the temperature configuration (85,0) yields no output at the lower portion in Fig. 13, signifying the emancipation from top-to-bottom coupling.

In summary, the visual representations and tabulated data collectively elucidate the intricacies of temperature coupling and the consequential impact of distinct decoupling strategies on the dynamic behavior of the tower. As can be seen in Fig. 9, after diagonal decoupling, the coupling is released, and the temperature at the top and bottom of the tower reaches the preset value, and the effect is obvious. As can be seen in Fig. 10, after feed forward compensation decoupling, the base of the tower reaches the preset value, while the top of the tower does not reach the preset value, which is lower than the preset value. Therefore, as can be seen from Fig. 9-10, the decoupling effect is obviously not as good as the diagonal decoupling effect during the simulation of the system.

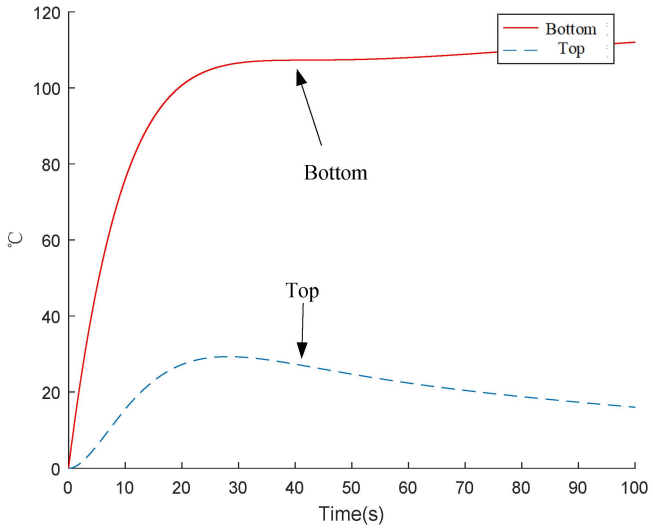

Fig. 6 Tower bottom to tower top coupling simulation diagram.

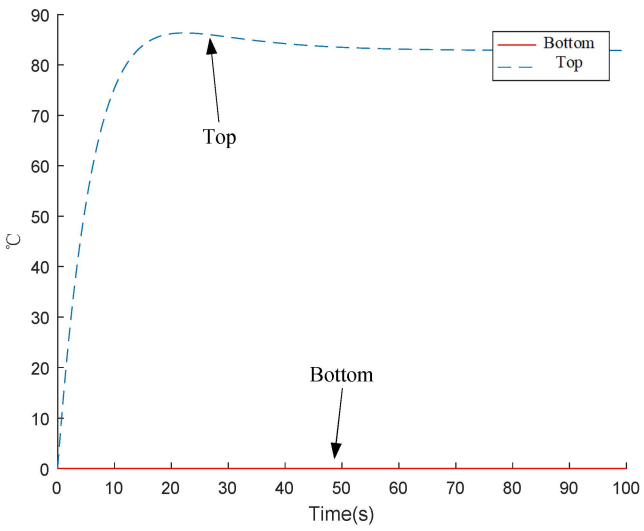

Fig. 9 Simulation of tower-to-bottom coupling after diagonal decoupling.

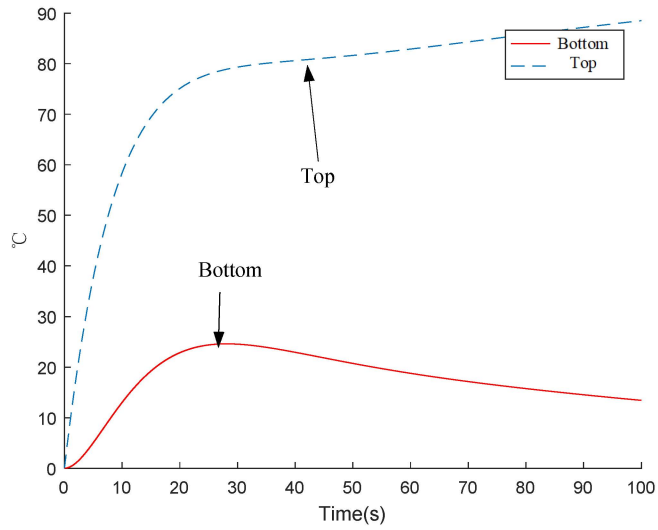

Fig. 7 Tower tower top to bottom coupling simulation diagram.

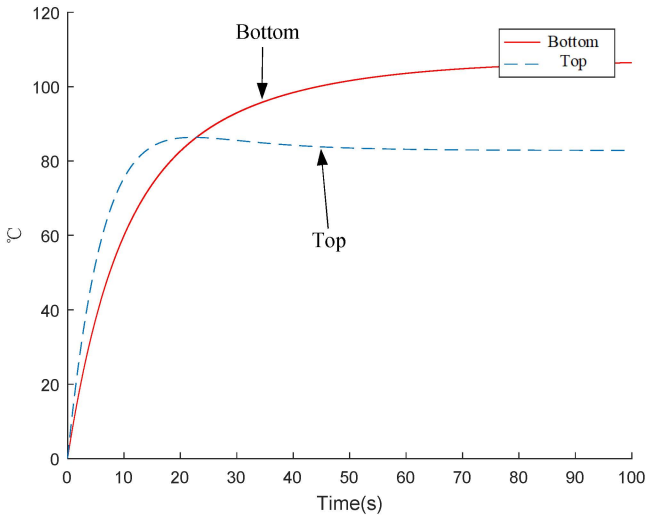

Fig. 10 Diagonal matrix decoupling simulation.

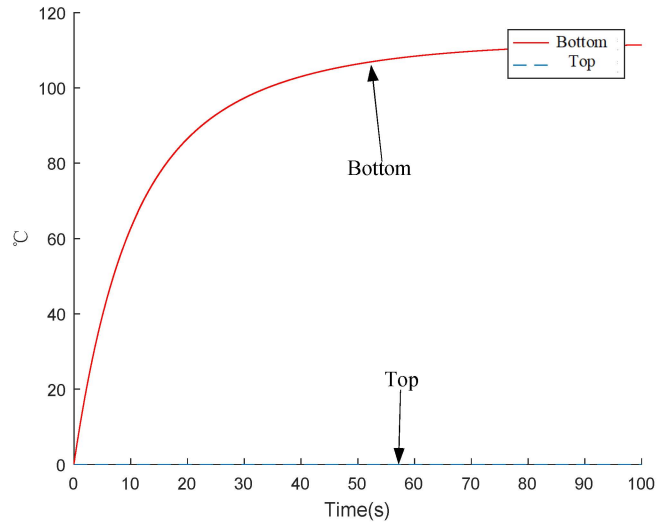

Fig. 8 Simulation diagram of coupling of tower bottom to tower top after diagonal decoupling.

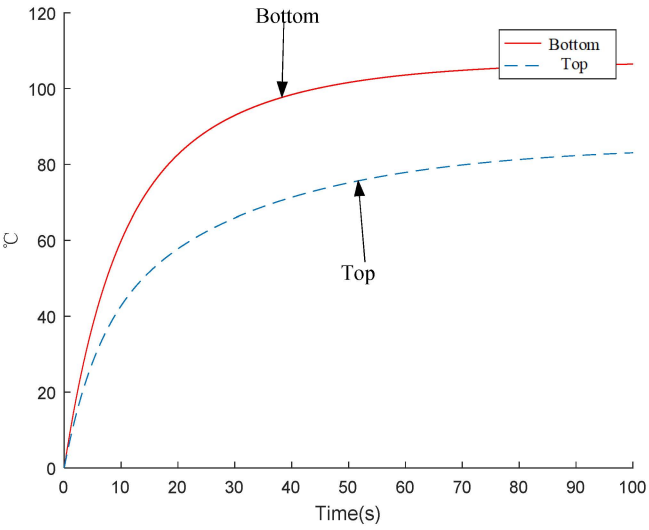

Fig. 11 Feed forward compensation decoupling simulation diagram.

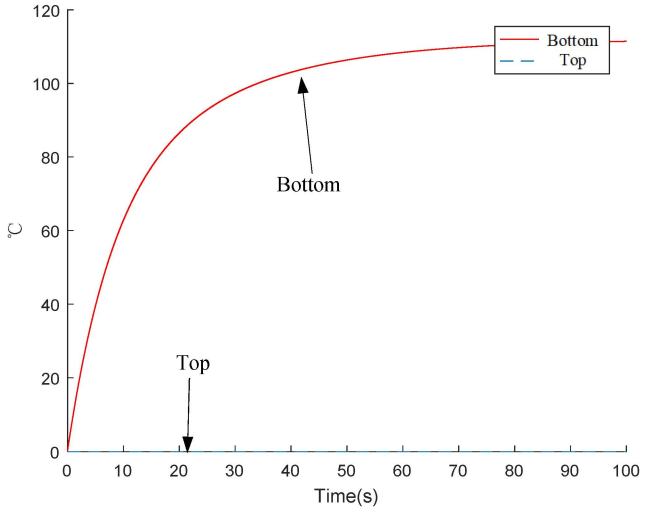

Fig. 12 Simulation of tower-to-tower coupling after feed forward compensation decoupling.

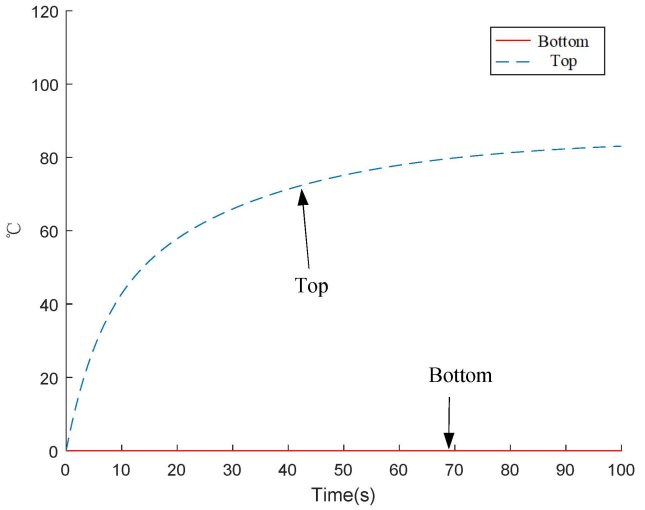

Fig. 13 Simulation of coupling top to bottom after feed forward compensation decoupling.

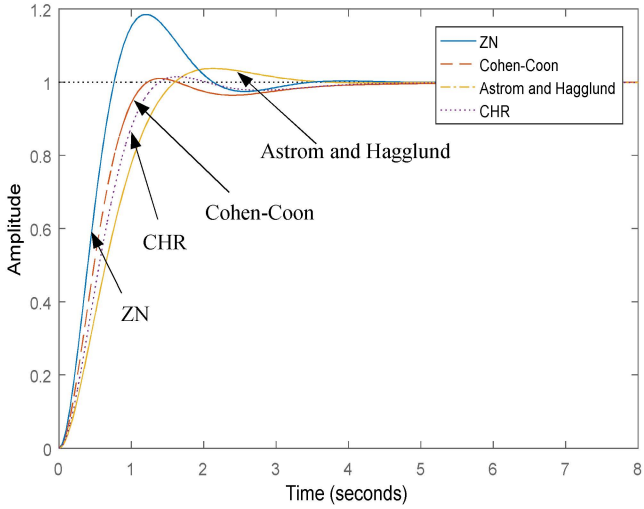

Fig. 14 Simulation results of four parameter tuning methods (tower temperature).

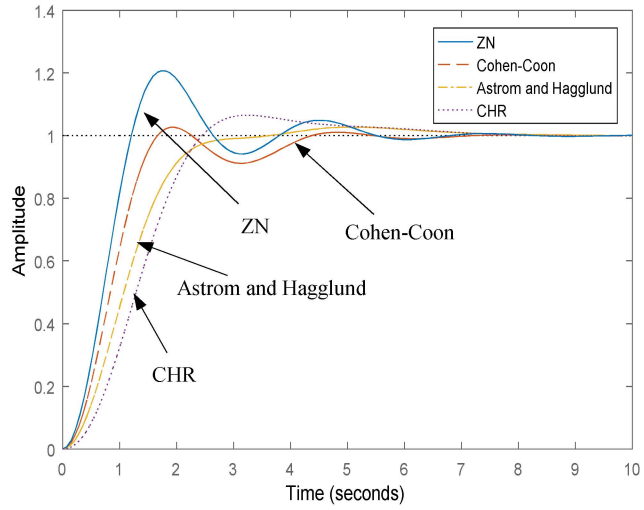

Fig. 15 Simulation results of four parameter tuning methods (bottom temperature).

Table VI. PID controller tuning parameters

PID Parameter tuning	Object 1			Object 2		
	K_p	K_i	K_d	K_p	K_i	K_d
ZN	1.7252	1.6212	0.7254	0.7156	0.6731	0.2756
C-C	0.7556	0.5189	0.8965	1.4142	0.7692	0.4635
A-H	0.3433	0.3555	0.4900	0.7642	0.8651	0.4702
CHR	0.2659	0.6953	0.2265	0.6599	0.7985	0.4996

Table VII. PID controller performance indicators

PID Performance index	Object 1				Object 2			
	ZN	C-C	A-H	CHR	ZN	C-C	A-H	CHR
O_s /%	19.41	1.51	1.31	2.36	21.24	3.21	1.65	2.65
T_r /s	1.26	1.44	1.39	1.89	1.74	1.69	2.41	2.19
T_s /s	2.27	2.48	2.51	2.37	2.07	2.11	2.5	2.66

VII. Conclusions

This paper analyzes the process of subspace identification from the structure and principle, uses subspace modeling combined with field data to model the PVC stripping system, introduces the decoupling algorithm commonly used in the current temperature coupling system, uses diagonal matrix method and feed forward compensation method to decouple the stripping system, and studies the PID control algorithm. Using Z-N frequency response method, Cohen-Coon method, Astrom and Hagglund method and CHR tuning four PID controller parameter engineering tuning methods were summarized on the basis of the PID control optimization of the decoupled system.

References

[1] W. Shi, J. Zhang, and X. M. Shi. "Different Photodegradation Processes of PVC with Different Average Degrees of Polymerization," *Journal of Applied Polymer Science,* vol. 107, no. 1, pp. 528-540, 2008.

[2] S. M.Bidoki, and R. Wittlinger. "Environmental and Economical Acceptance of Polyvinyl Chloride (PVC) Coating Agents," *Journal of Cleaner Production,* vol. 18, no. 3, pp. 219-225, 2010.

[3] E. D. Comaniţă, C. Ghinea, and M. Roşca. "Environmental Impacts of Polyvinyl Chloride (PVC) Production Process," 2015 *E-Health and Bioengineering Conference (EHB). IEEE,* pp. 1-4, 2015.

[4] P. Lieberzeit, D. Bekchanov, and M. Mukhamediev. "Polyvinyl Chloride Modifications, Properties, and Applications," *Polymers for Advanced Technologies,* vol. 33, no. 6, pp. 1809-1820, 2022.

[5] T. Ahmad, and C. Guria. "Progress in the Modification of Polyvinyl Chloride (PVC) Membranes: A Performance Review for Wastewater Treatment," *Journal of Water Process Engineering,* vol. 45, pp. 102466, 2022.

[6] P. Marusak, and P. Tatjewski. "Effective Dual-mode Fuzzy DMC Algorithm with Quadratic Optimization and Guaranteed Stability," *International Journal of Applied Mathematics & Computer Science,* vol. 19, no. 1, pp. 127-141, 2009.

[7] P. Marusak, and P. Tatjewski. "Stability Analysis of Nonlinear Control Systems with Unconstrained Fuzzy Predictive Controllers," *Archives of Control Science,* vol. 12, no. 3, pp. 267-288, 2002.

[8] Y. Tian, J. Zhang, and J. Morris. "Modeling and Optimal Control of a Batch Polymerization Reactor Using a Hybrid Stacked Recurrent Neural Network Model," *Industrial & Engineering Chemistry Research,* vol. 40, no. 21, pp. 4525-4535, 2010.

[9] Y. Ye, B. Wang, and M. Shao. "Polymerizer Temperature Cascade Control System Based on Generalized Predictive Control," *Physics Procedia,* vol. 24, no. 1, pp. 184-189, 2012.

[10] F. Manenti, and M. Rovaglio. "Integrated Multilevel Optimization in Large-scale Poly (Ethylene Terephthalate) Plants," *Industrial & Engineering Chemistry Research,* vol. 47, no. 1, pp. 92-104, 2008.

[11] J. D. Fonseca, G. Grause, and T. Kameda. "Effects of Steam on the Thermal Dehydrochlorination of Poly (Vinyl Chloride) Resin and Flexible Poly (Vinyl Chloride) under Atmospheric Pressure," *Polymer Degradation and Stability*, vol. 117, no. 1, pp. 8-15, 2015.

[12] J. Liu. "The Application and Simulation Research of the Fuzzy PID Control Used in PVC Polymerization Temperature Control System," *Advanced Materials Research,* vol. 466-467, no. 1, pp. 47-51, 2012.

[13] M. A. Tooma, T. S. Najima, and Q. F. Alsalhy. "Modification of Polyvinyl Chloride (PVC) Membrane for Vacuum Membrane Distillation (VMD) Application," *Desalination,* vol. 373, no. 1, pp. 58-70, 2015.

[14] S. Gao, J. Yang, and J. Wang. "D-FNN Based Modeling and BP Neural Network Decoupling Control of PVC Stripping Process," *Mathematical Problems in Engineering,* vol. 2014, pp. 681259, 2014.

[15] H. Y. Wang, D. Wei, and J. S. Wang. "Modeling Method Based on Output-layer Structure Feedback Elman Neural Network and PID Decoupling Control of PVC Stripping Process," *IAENG International Journal of Computer Science,* vol. 47, no. 4, pp. 623-633, 2020.

[16] S. Tuhta, F. Günday, and H. Aydin. "Mimo System Identification of Machine Foundation Using N4SID," *International Journal of Interdisciplinary Innovative Research Development,* vol. 4, no. 1, pp. 27-36, 2019.

[17] P. Falb, and W. Wolovich. "Decoupling in the Design and Synthesis of Multivariable Control Systems," *IEEE Transactions on Automatic Control,* vol. 12, no. 6, pp. 651-659, 1967.

[18] K. Peng, H. Wang, and H. Zhang. "Multivariable Decoupling Control of Civil Turbofan Engines Based on Fully Actuated System Approach," *Journal of Systems Science and Complexity,* vol. 36, no. 3, pp. 947-959, 2023.

[19] S. M. Attaran, R. Yusof, and H. Selamat. "Enhancement of Control's Parameter of Decoupled HVAC System via Adaptive Controller Through the System Identification Tool Box," *Jurnal Teknologi*, vol. 76, no. 1, pp. 261-272, 2015.

[20] Y. Wang, Z. Chen, and Y. Jiang. "High-Order Neural-Network-Based Multi-Model Nonlinear Adaptive Decoupling Control for Microclimate Environment of Plant Factory," *Sensors*, vol. 23, no. 19, pp. 8323, 2023.

[21] F. Xu, D. Li, and Y. Xue. "Comparative Study of PID Parameter Tuning Method Based on ITAE Index," *Chinese Journal of Electrical Engineering*, vol. 23, no. 8, pp. 206-210, 2003.